Thickness-dependent twinning evolution and ferroelectric behavior of epitaxial $BiFeO_3$ (001) thin films

Huajun Liu,[1,2] Kui Yao,[2] Ping Yang,[3] Yonghua Du,[4] Qing He,[5] Yueliang Gu,[5] Xiaolong Li,[5] Sisheng Wang,[5] Xingtai Zhou,[5] and John Wang[1,*]

[1]*Department of Materials Science and Engineering, National University of Singapore, Singapore 117574, Singapore*

[2]*Institute of Materials Research and Engineering, A*STAR (Agency for Science, Technology and Research), Singapore 117602, Singapore*

[3]*Singapore Synchrotron Light Source (SSLS), National University of Singapore, 5 Research Link, Singapore 117603, Singapore*

[4]*Institute of Chemical and Engineering Sciences, A*STAR (Agency for Science, Technology and Research), 1 Pesek Road, Jurong Island, Singapore 627833, Singapore*

[5]*Shanghai Synchrotron Radiation Facility (SSRF), Shanghai Institute of Applied Physics, Chinese Academy of Sciences, 239 Zhangheng Road, Shanghai 201204, People's Republic of China*

(Received 13 May 2010; revised manuscript received 19 July 2010; published 19 August 2010)

With increasing film thickness of the epitaxial $BiFeO_3$ (001) films deposited on $SrTiO_3$ substrates from 30 to 720 nm, the crystal structure evolutes from a fully strained tetragonal lattice to partially relaxed monoclinic one with rotated twins. Although the mismatch strain results in a significant lattice distortion and twinning evolution, the polarization does not show a direct correlation with strain. Instead, there is a strong dependence of polarization on the body diagonal length of the distorted pseudocubic unit cell. The distortion in the polarization direction is the critical parameter, other than strain, that determines the polarization in the monoclinic phase ferroelectric thin films.

DOI: 10.1103/PhysRevB.82.064108 PACS number(s): 73.40.Lq, 77.84.−s, 85.50.Gk, 77.80.−e

I. INTRODUCTION

Ferroelectric thin films promise wide applications in microelectronic and data-storage devices, such as sensors, transistors, and nonvolatile memories.[1] Exploring how the substrate-induced strain affects the ferroelectric behavior of ferroelectric thin films is an important issue, as epitaxial strains can dramatically enhance the ferroelectric polarization and Curie temperature of thin films compared to their bulk counterparts. For example, the epitaxial strain has been shown to produce room-temperature ferroelectricity in $SrTiO_3$ thin films by increasing the ferroelectric transition temperature (T_C) for several hundreds of degrees.[2] In $BaTiO_3$ epitaxial thin films, strain gives rise to a T_C nearly 500 °C higher and a remanent polarization 250% higher than those of bulk single crystal.[3] Therefore, due to the strong coupling between ferroelectric order and strain, ferroelectric properties can be tuned by a proper control of epitaxial strain.

$BiFeO_3$ (BFO) has attracted great attention in recent years, as it is a single-phase multiferroic material at room temperature.[4,5] Bulk BFO exhibits a rhombohedrally distorted perovskite structure with space group $R3c$ and lattice parameters $a=3.96$ Å and $\alpha=89.4°$.[6] The spontaneous polarization in bulk BFO is along the [111] direction in pseudocubic unit cell and the value calculated from the first-principles is 90–100 $\mu C/cm^2$.[7] In the case of epitaxial BFO thin films grown under compressive strain, the lattice will be deformed, which can be tetragonal or monoclinic dependent on film thickness and deposition techniques.[8] Recently, a strain-driven morphotropic phase boundary was demonstrated in BFO films grown on $LaAlO_3$ (001) substrate, showing the dramatic effect of strain engineering in BFO thin films.[9]

There have been a lot of works about the strain effect on the polarization of BFO epitaxial thin films. For example, for rhombohedral phase BFO ($R3c$), the first-principles calculation has showed that the dependence of polarization on epitaxial strain is very weak.[10] Later, large spontaneous polarization, which is comparable with that of epitaxial thin film, has also been obtained in strain-free bulk single crystal.[11] The experimental results reported by Kim *et al.*[12] have demonstrated that indeed the polarization almost keep unchanged when strain relaxes with increasing film thickness of (001) BFO films grown on $SrTiO_3$ (STO) substrate. More recently, Jang *et al.*[13] have confirmed that the spontaneous polarization itself keep unchanged while there was a strong strain dependence of polarization in BFO (001) thin films due to the polarization rotation. Therefore, the strain effect on polarization in BFO epitaxial thin films is rather negligible. On the other hand however, the lattice of a BFO film is distorted by epitaxial strain, which would, in principle, affect the dipole moment therefore the polarization as in other ferroelectric thin films.[2,3] In this paper, we demonstrate that the epitaxial BFO (001) film with twinning rotation structure shows a large variance of polarization up to 58% as the film thickness changes, strongly depending on the length of polarization direction along the body diagonal.

II. METHODOLOGY

In our previous work on the epitaxial BFO (001) film grown on (001) STO with 60 nm $SrRuO_3$ (SRO) buffer layer, a twinning rotation structure was identified, which greatly decreases the leakage current and improves remanent polarization.[14] In order to investigate the effect of residual strain on twinning evolution and ferroelectric behavior, epitaxial BFO (001) films with thickness from 30 to 720 nm were grown by radio-frequency sputtering. The crystal structure was identified by high-resolution synchrotron x-ray diffractometry at the XDD beam line of Singapore Synchrotron

 ©2010 The American Physical Society

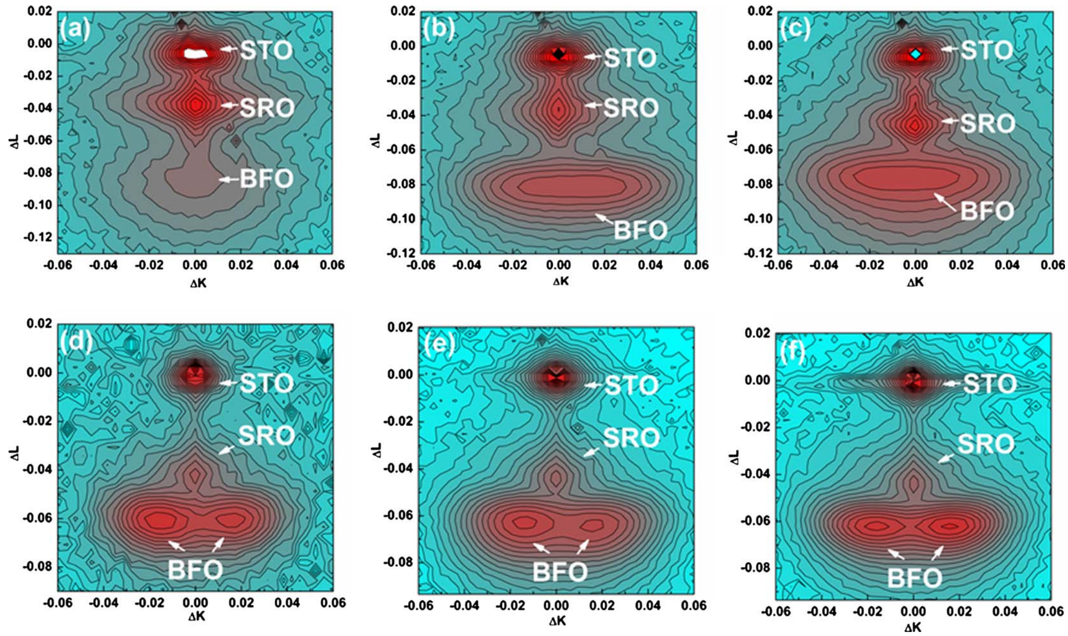

FIG. 1. (Color online) *KL* reciprocal space mappings around $SrTiO_3$ (002) for the epitaxial $BiFeO_3$ films with film thickness of (a) 30 nm, (b) 180 nm, (c) 360 nm, (d) 450 nm, (e) 540 nm, and (f) 720 nm, respectively.

Light Source (SSLS) and BL14B1 beam line of Shanghai Synchrotron Radiation Facility (SSRF), using 1.000 Å x-rays with a Huber 5021 six-axes diffractometer. The ferroelectric and leakage behavior of the thin film were investigated by using the radiant precise workstation (Radiant Technologies) and Keithley 6430 *I*-*V* system, respectively. The experimental details for sample preparation were described elsewhere.[14]

III. RESULTS AND DISCUSSION

Figure 1 shows the *KL* reciprocal space mappings (RSM) from (002) STO diffraction of the epitaxial BFO thin films (*H*, *K*, and *L* are reciprocal space coordinates). The vertical axis is along the *L* direction while the horizontal axis is along *K* direction in the reciprocal space. The spots from STO and SRO remain to be a single peak for all mappings with dif-

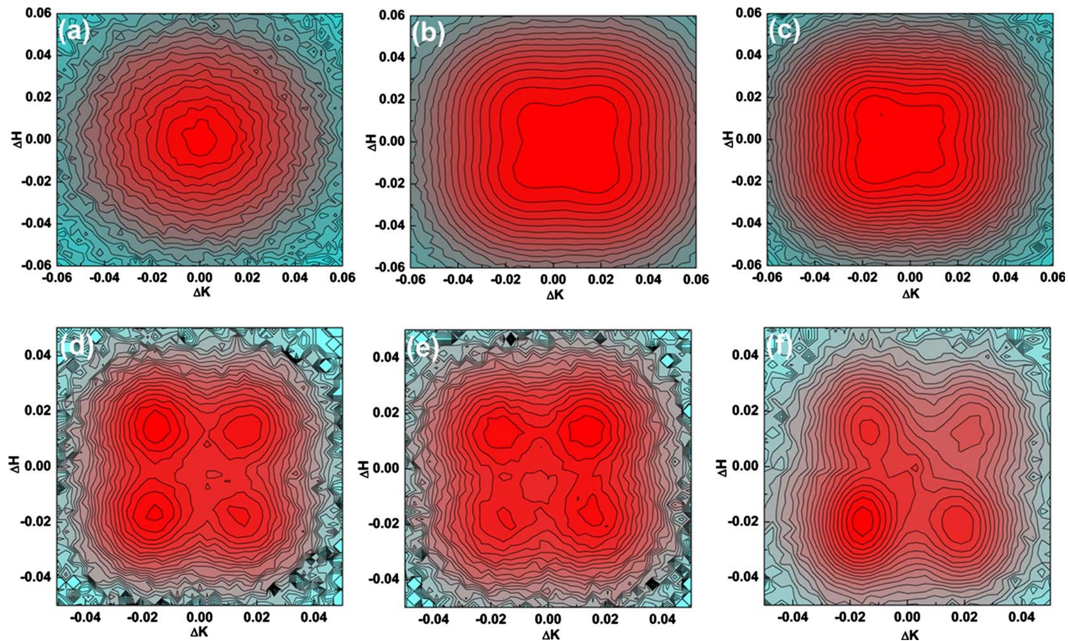

FIG. 2. (Color online) *KH* reciprocal space mappings around $SrTiO_3$ (002) for the epitaxial $BiFeO_3$ films with film thickness of (a) 30 nm, (b) 180 nm, (c) 360 nm, (d) 450 nm, (e) 540 nm, and (f) 720 nm, respectively. *L* values were set at corresponding BFO peaks in Fig. 1.

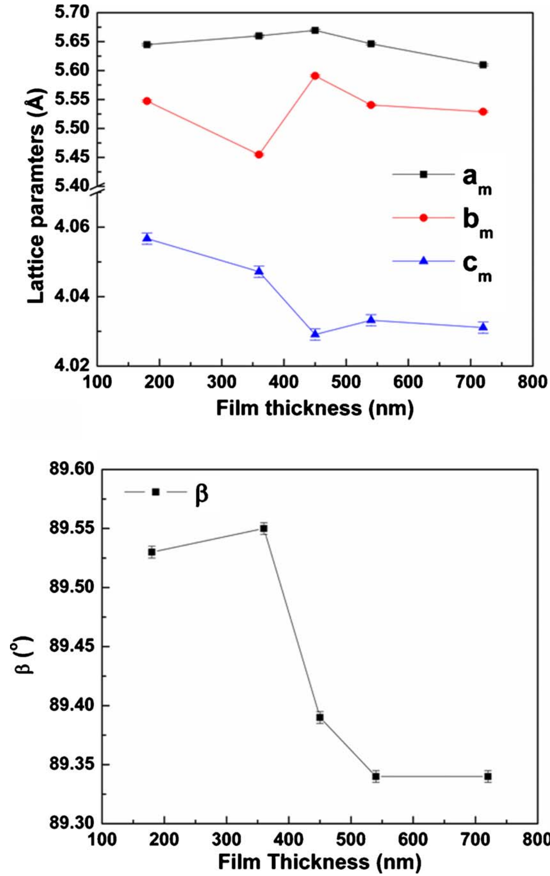

FIG. 3. (Color online) Lattice parameters derived from reciprocal space mappings for the epitaxial $BiFeO_3$ film with the film thickness changing from 180 to 720 nm.

ferent film thicknesses, showing a high quality of epitaxial growth of the SRO buffer layer. However, for the diffraction peaks from BFO, it develops from a single sharp peak at 30 nm to an elongated peak at 180 and 360 nm, and finally to two well-separated peaks for 450, 540, and 720 nm films. As discussed in Ref. 14, these two peaks with the same L value indicate a rotated twinning structure in BFO lattice. Therefore, with increasing film thickness, the BFO film changes from a strained lattice to a partially relaxed one with monoclinic rotated twinning structure.

In order to fully understand the crystal structure of the BFO films of varying thicknesses, KH (H, K, and L are reciprocal space coordinates) RSM around (002) STO diffraction were measured for BFO thin films with thickness changing from 30 to 720 nm, as shown in Fig. 2. These mappings were obtained with L value at the BFO peaks in Fig. 1. Clearly, for the 30 nm film, a single peak without any distortion was observed. As the film thickness increases, the BFO spot shows a trend to form four peaks for diffraction in the KH plane. This confirms the structure model proposed in Ref. 14, in which two pairs of twin variants along [100] and [010] coexist.

From the reciprocal space mappings shown above and the mappings around (103) and (113) (not shown here), the crystal structures and lattice parameters were determined, as summarized in Fig. 3. The BFO film possesses a fully strained tetragonal structure for the film with thickness of 30 nm. However, the films with thickness increasing from 180 to 720 nm show a monoclinic twinning structure, which is initiated at 180 nm and fully developed at 450 nm. The monoclinic distortion angle β shows increasing deviation from 90° as film thickness increases. The lattice parameters exhibit a different evolution as compared to the film with in-plane twins but without out-of-plane twinning rotation.[15] This unique out-of-plane twinning rotation relaxes strain in the films and maintains a degree of distortion in lattice parameters even at a film thickness of 720 nm.

Figure 4(a) shows the hysteresis loops for the 180 and 450 nm BFO thin films at the frequency of 3 kHz. Both loops are squarelike, showing the intrinsic remanent polarizations of epitaxial ferroelectric thin films. Due to the large leakage current, the polarization of 30 nm film cannot be properly measured. The polarization as a function of BFO film thickness increasing from 180 to 720 nm is plotted in Fig. 4(b). The remanent polarization increases from 55 to 87 $\mu C/cm^2$ when the film thickness increases from 180 to 450 nm, representing about 58% enhancement. As reported in Ref. 11, for epitaxial BFO (001) films without twinning rotation structure, the polarization is almost unchanged as the film thickness increases from 77 to 960 nm. This great enhancement of polarization observed in the present work is thus related to the unique strain relaxation mechanism by twinning rotation. Figure 4(c) shows the leakage current density of the epitaxial BFO (001) film as a function of applied electrical field for film thickness from 180 to 720 nm. The leakage current density measured at 100 kV/cm is plotted as a function of film thickness in Fig. 4(d). Despite that the 180 nm film has a larger leakage current than others; all the samples show very low leakage current on the order of 10^{-6} A/cm^2. This agrees with the squarelike loops obtained in ferroelectric hysteresis test and confirms the intrinsic polarization measured.

The monoclinic lattice of BFO is orientated by 45° with respect to [001] direction of the substrate. A schematic configuration of monoclinic unit cell is represented by the thick lines in Fig. 5(a) while the pseudocubic (pc) unit cell is shown by the dashed lines. In order to derive the in-plane strain, the lattice parameters of monoclinic unit cell have to be transformed into the pseudocubic cell. This relation is given by

$$a_{\mathrm{film}} = \frac{a_m + b_m}{2\sqrt{2}}, \tag{1}$$

$$c_{\mathrm{film}} = c_m / \sin \beta, \tag{2}$$

where a_{film} and c_{film} are the lattice constants for the pseudocubic cell. As the thin SRO buffer layer and STO substrate are rather close in lattice parameters, as compared to that between BFO and STO, the mismatch strain is largely arising from the lattice mismatch between the BFO film and STO substrate. Taking the bulk BFO rhombohedral phase as reference, the in-plane and out-of-plane strain is calculated by the following relationship:

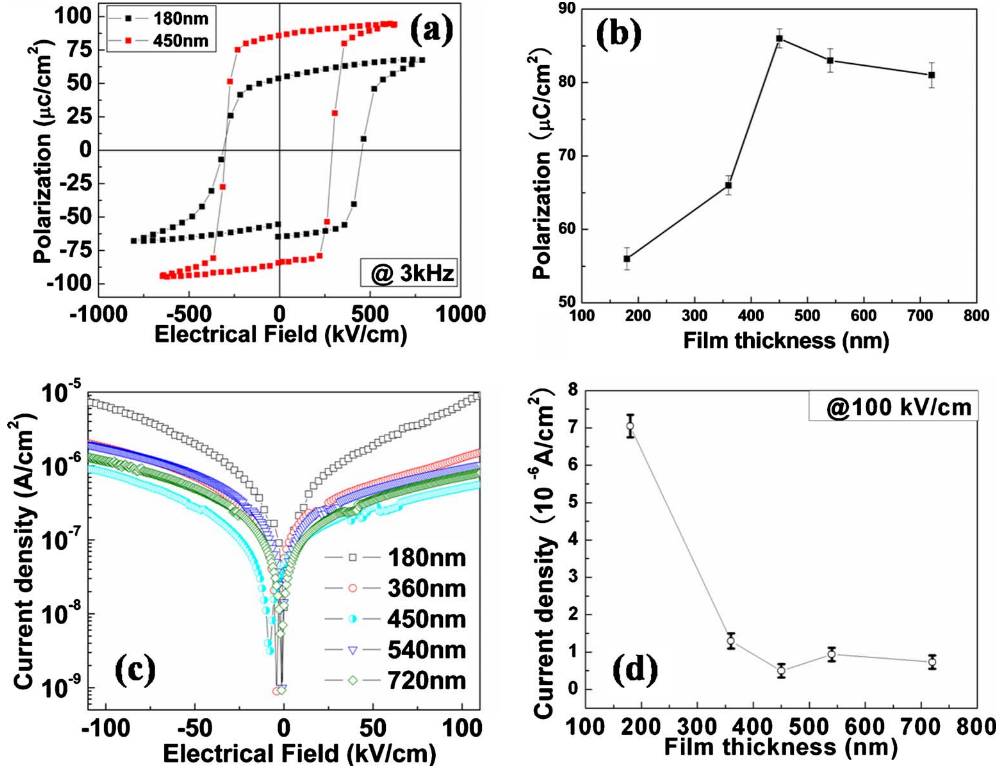

FIG. 4. (Color online) (a) Hysteresis loops for epitaxial $BiFeO_3$ thin films of 180 and 450 nm in thickness; (b) remanent polarization as a function of film thickness; (c) *J-E* relationships of the Au/BFO/SRO capacitor for the epitaxial $BiFeO_3$ film with film thickness increasing from 180 to 720 nm; and (d) leakage current density at 100 kV/cm as a function of film thickness from 180 to 720 nm.

$$\varepsilon_{\text{in-plane}} = \varepsilon_{xx} = \varepsilon_{yy} = \frac{a_{\text{film}} - a_{\text{bulk}}}{a_{\text{bulk}}}, \quad (3)$$

$$\varepsilon_{\text{out-of-plane}} = \varepsilon_{zz} = \frac{c_{\text{film}} - c_{\text{bulk}}}{c_{\text{bulk}}}. \quad (4)$$

The strains thus derived are plotted as a function of film thickness in Fig. 5(b). The in-plane strain does not relax from negative to zero with increasing thickness as expected but varies slightly from −0.5% to +0.5%. This unique behavior of strain evolution is due to the twinning rotation. At 180 nm film thickness, when the twinning is initiated, the compressive strain is relaxed to nearly zero. While, the fully developed twinning rotation structure even drives the compressive strain from the substrate to be tensile at 450 nm. For the out-of-plane strain, it keeps decreasing as the film becoming thicker, except a drop at 450 nm when the twinning rotation is fully formed. The trend of strain change does not agree with the change in polarization in Fig. 4(b), showing no direct correlation between the residual strain and polarization. This agrees with the result of the first-principles calculations[10] and previous experimental results[12] that the polarization of BFO is not strongly dependent on the strain. In addition, the polarization rotation mechanism proposed in Ref. 13 also cannot explain the polarization change of about 58% observed in our films. For the 450 nm BFO film with a tensile in-plane strain, the rotation of polarization is expected to toward $[110]_{pc}$ and give rise to lower polarization along the measured [001] direction. However, the polarization measured at 450 nm is even higher than those with compressive in-plane strain.

If the strain is not the critical parameter to account for the large polarization variance with film thickness, then now we turn to the length of polarization direction along the body diagonal of pseudocubic lattice. As is shown by the dashed line $[111]_{pc}$ in Fig. 5(a), the body diagonal direction is the face diagonal of (101) in monoclinic cell. The calculated length along $[111]_{pc}$ and polarization are plotted in Fig. 6 as a function of film thickness. A strong and clear dependence of polarization on the $[111]_{pc}$ length is obviously seen. For the ferroelectric film of tetragonal phase, the in-plane strain is very important as it affects the length of polarization direction in [001]. Indeed, the first-principles study shows tetragonal phase ferroelectric films [$BaTiO_3$, $PbTiO_3$ and $BiFeO_3$ (*P*4*mm*)] are in-plane strain sensitive.[10] However, for the monoclinic phase, the in-plane strain is not the critical influencing factor, because the polarization direction is not along [001] any more. Although the monoclinic phase of our BFO films shows a degree of distortion from the bulk rhombohedral phase, the polarization direction should still be along the body diagonal direction in pseudocubic unit cell. Therefore, the body diagonal length is the determining factor, as it affects the space for the ionic displacement within the unit cell.

IV. SUMMARY

By employing high resolution x-ray diffraction, twinning evolution was shown for epitaxial BFO (001) films grown on

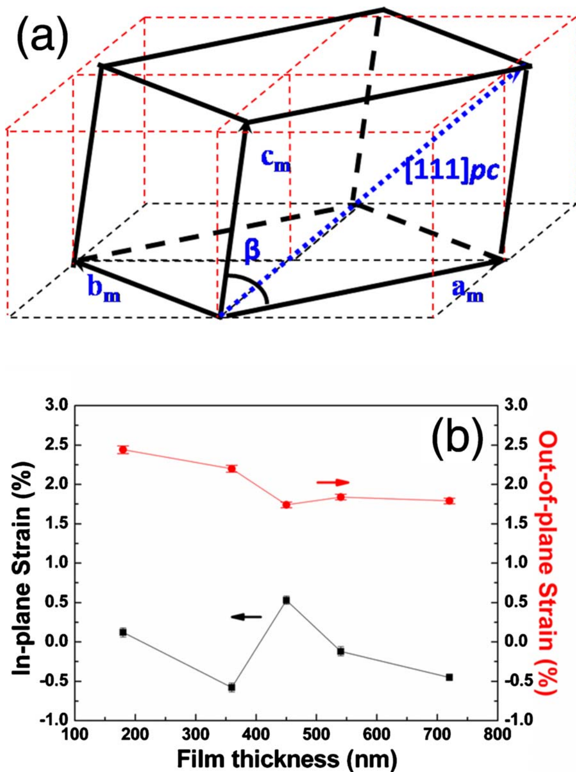

FIG. 5. (Color online) (a) A schematic drawing for the relationship between monoclinic unit cell (thick lines) and pseudocubic unit cell (dashed lines) and (b) in-plane strain and out-of plane strain as a function of film thickness.

(001) STO with SRO buffer layer. The lattice parameters and epitaxial strain derived from reciprocal space mapping show significant lattice distortions. Polarization has a strong dependence on the body diagonal length of distorted pseudocubic unit cell. While in conventional perovskite ferroelectric materials with tetragonal phase, in-plane strain can turn the polarization greatly; our results indicate that more attention should be paid to the distortion in polarization direction along body diagonal in monoclinic phase ferroelectric thin films.

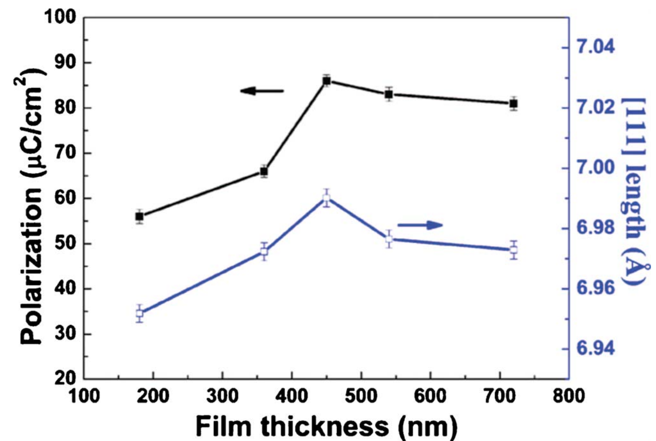

FIG. 6. (Color online) Remanent polarization and $[111]_{pc}$ length as a function of film thickness.

ACKNOWLEDGMENTS

The authors would like to thank the support from SSLS via NUS Core Support under Grant No. C-380-003-003-001, A*STAR/MOE under Grant No. RP 397990 8M, A*STAR under Grant No. 012 105 0038, A*STAR under Grants No. R144-000-053-303 and No. ARF R-144-000-53-107, and A*STAR under Grant No. 012 101 0131. The authors would also like to thank BL14B1 (diffraction) and BL14W1 (XAFS) beam lines of Shanghai Synchrotron Radiation Facility (SSRF) for technical support. This work is partly funded by National Natural Science Foundation of China under Grant No. 10979073.

*Author to whom correspondence should be addressed; msewangj@nus.edu.sg

[1] M. Dawber, K. M. Rabe, and J. F. Scott, Rev. Mod. Phys. **77**, 1083 (2005).

[2] J. H. Haeni, P. Irvin, W. Chang, R. Uecker, P. Reiche, Y. L. Li, S. Choudhury, W. Tian, M. E. Hawley, B. Craigo, A. K. Tagantsev, X. Q. Pan, S. K. Streiffer, L. Q. Chen, S. W. Kirchoefer, J. Levy, and D. G. Schlom, Nature (London) **430**, 758 (2004).

[3] K. J. Choi, M. Biegalski, Y. L. Li, A. Sharan, J. Schubert, R. Uecker, P. Reiche, Y. B. Chen, X. Q. Pan, V. Gopalan, L. Q. Chen, D. G. Schlom, and C. B. Eom, Science **306**, 1005 (2004).

[4] J. Wang, J. B. Neaton, H. Zheng, V. Nagarajan, S. B. Ogale, B. Liu, D. Viehland, V. Vaithyanathan, D. G. Schlom, U. V. Waghmare, N. A. Spaldin, K. M. Rabe, M. Wutting, and R. Ramesh, Science **299**, 1719 (2003).

[5] G. Catalan and J. F. Scott, Adv. Mater. **21**, 2463 (2009).

[6] F. Kubel and H. Schmid, Acta Crystallogr., Sect. B: Struct. Sci. **46**, 698 (1990).

[7] J. B. Neaton, C. Ederer, U. V. Waghmare, N. A. Spaldin, and K. M. Rabe, Phys. Rev. B **71**, 014113 (2005).

[8] K. Saito, A. Ulyanenkov, V. Grossmann, H. Ress, L. Bruegemann, H. Ohta, T. Kurosawa, S. Ueki, and H. Funakubo, Jpn. J. Appl. Phys., Part 1 **45**, 7311 (2006).

[9] R. J. Zeches, M. D. Rossell, J. X. Zhang, A. J. Hatt, Q. He, C. H. Yang, A. Kumar, C. H. Wang, A. Melville, C. Adamo, G. Sheng, Y. H. Chu, J. F. Ihlefeld, R. Erni, C. Ederer, V. Gopalan, L. Q. Chen, D. G. Schlom, N. A. Spaldin, L. W. Martin, and R. Ramesh, Science **326**, 977 (2009).

[10] C. Ederer and N. A. Spaldin, Phys. Rev. Lett. **95**, 257601 (2005).

[11] D. Lebeugle, D. Colson, A. Forget, and M. Viret, Appl. Phys. Lett. **91**, 022907 (2007).

[12] D. H. Kim, H. N. Lee, M. D. Biegalski, and H. M. Christen, Appl. Phys. Lett. **92**, 012911 (2008).

[13] H. W. Jang, S. H. Baek, D. Ortiz, C. M. Folkman, R. R. Das, Y. H. Chu, P. Shafer, J. X. Zhang, S. Choudhury, V. Vaithy-

anathan, Y. B. Chen, D. A. Felker, M. D. Biegalski, M. S. Rzchowski, X. Q. Pan, D. G. Schlom, L. Q. Chen, R. Ramesh, and C. B. Eom, Phys. Rev. Lett. **101**, 107602 (2008).
[14] H. Liu, P. Yang, K. Yao, and J. Wang, Appl. Phys. Lett. **96**, 012901 (2010).
[15] C. J. M. Daumont, S. Farokhipoor, A. Ferri, J. C. Wojdel, Jorge Iniguez, B. J. Kooi, and B. Noheda, Phys. Rev. B **81**, 144115 (2010).